

# Fabrication of Titanium Dioxide Nanorod Arrays-Polyaniline Heterojunction for Development of UV Photosensor

M.M. Yusoff<sup>1,5,\*</sup>, M.H. Mamat<sup>1,2,\*</sup>, M.F. Malek<sup>1</sup>, N. Othman<sup>1</sup>, A.S. Ismail<sup>1</sup>, S.A. Saidi<sup>1</sup>, R. Mohamed<sup>3</sup>, A.B. Suriani<sup>4</sup>, Z. Khusaimi<sup>2</sup> and M. Rusop<sup>1,2</sup>

<sup>1</sup>NANO-ElecTronic Centre, Faculty of Electrical Engineering, Universiti Teknologi MARA, 40450 Shah Alam, Selangor, Malaysia

<sup>2</sup>NANO-SciTech Centre, Institute of Science, Universiti Teknologi MARA, 40450 Shah Alam, Selangor, Malaysia

<sup>3</sup>Faculty of Applied Sciences, Universiti Teknologi MARA Pahang, 26400 Jengka, Pahang, Malaysia

<sup>4</sup>Faculty of Science and Mathematics, Universiti Pendidikan Sultan Idris, Tanjung Malim, Perak 35900, Malaysia

<sup>5</sup>Kulliyah of Engineering, International Islamic University Malaysia (IIUM), 50728, Kuala Lumpur, Malaysia

**Abstract:** An ultraviolet (UV) photosensor is successfully fabricated via heterojunction device consisted of n-type titanium dioxide (TiO<sub>2</sub>) nanorod arrays (TNAs), and p-type polyaniline (PANI) by a facile method on fluorine tin oxide (FTO)-coated glass substrate. The fabricated UV photosensor demonstrated a UV-catalyst activity through the generation of photocurrent under UV irradiation (365 nm, 750 μW/cm<sup>2</sup>). The measured UV response showed the highest generation of photocurrent of 0.52 μAcm<sup>-2</sup>, and responsivity of 0.65 mA/W at 1.0 V reverse bias. The results indicate that the fabricated TNAs/PANI heterojunction-based device could be a promising candidate for the application of UV photosensor.

**Keywords:** TiO<sub>2</sub> nanorod, TNAs/PANI heterojunction, UV photosensor, Optical materials, Electronic materials.

## 1. INTRODUCTION

Ultraviolet (UV) photosensor has been considered to attract various investigations lately due to its wide applications scientifically in military, solar astronomy, UV scanning, fire detection and environmental researches [1-3]. Particularly, heterojunction structure is one of the method suggested for the detection of UV irradiation in attribution to its ability to regulate the mobility of the photo-generated charge carriers and causes the generation of photocurrent for sensing system. Recently, nanomaterials-based semiconductor such as TiO<sub>2</sub>, ZnO, SnO<sub>2</sub>, ZnS, GaN, BiOBr, Ga<sub>2</sub>O<sub>3</sub> and others have been widely studied for the applications of UV photosensor [4-12]. Many studies have been focusing on nanostructured TiO<sub>2</sub> material due to its many advantages including low cost, earth abundance, non-toxicity, physical and chemical stability and enhanced optoelectronic properties [13-16]. However, the methods used for synthesizing and depositing the TiO<sub>2</sub> layer are complex and very lengthy processes. Therefore, an improvement on current methods to more simple, rapid, and consistent process

need to be studied for the deposition of TiO<sub>2</sub> on the substrate. Herein, we present a novel one-step immersion method to deposit TiO<sub>2</sub> nanorod arrays (TNAs) on fluorine tin oxide (FTO)-coated glass substrate.

The use of glass container in our study was deliberately to replace the use of stainless steel-based autoclave for the deposition of thin film TNAs at low temperature and growth time. The deposited TNAs was used to fabricate a UV photosensor based on heterostructured TNAs/PANI. The fabricated composite layers exhibited excellent UV sensing and switching properties.

## 2. MATERIALS AND METHODS

N-type TNAs was synthesized and deposited using a novel facile immersion method in a Schott bottle on FTO-coated glass substrate for 2 hours at 150 °C, as reported in our previous work [17]. To begin this process, FTO-coated glass substrate was cleaned with acetone, ethanol, and deionized (DI) water for 10 minutes subsequently in an ultrasonic bath (Hwasin Technology PowerSonic 405, 40 kHz). A solution comprising HCl (37 %, Merck) and DI water in 1:1 volume ratio was added in a Schott bottle, and stirred. Once the solution was stirred for 10 minutes, 0.07 M of

\*Address correspondence to this author at the NANO-ElecTronic Centre, Faculty of Electrical Engineering, Universiti Teknologi MARA, 40450 Shah Alam, Selangor, Malaysia;  
Tel: +60355211883; Fax: +60355443870;  
E-mail: mhmatat@salam.uitm.edu.my; eezeehiro@gmail.com

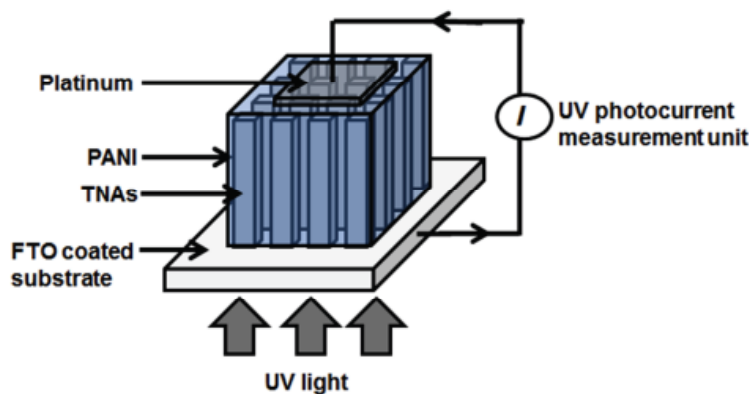


**Figure 1:** Schematic Structure of TNAs/PANI heterojunction- based UV photosensor.

titanium (IV) butoxide (97%, Sigma-Aldrich) was gently added in the solution and continuously stirred for another 30 minutes. The prepared substrate was then immersed in the solution with the conductive side facing upward in the bottle. The bottle was then tightly sealed and heated in an oven. After the growth process was completed, the deposited substrate containing TNAs was taken out from the bottle and rinsed with DI water and dried at room temperature. Finally, the deposited substrate was annealed in a furnace at 450 °C for 30 minutes.

P-type PANI [18] from aniline (99 %, Sigma-Aldrich) was then deposited on the TNAs layer on the prepared substrate via spin coating method. Finally, a layer of platinum (Pt) of 90 nm thickness was deposited on the PANI layer, as back contact of the fabricated heterojunction-based UV photosensor by thermal evaporator (TE, ULVAC). The device structure is shown in Figure 1.

The effective area was designed approximately of 1.0 cm<sup>2</sup> at the centre of photosensor device. The characterization of fabricated heterojunction-based UV photosensor was performed via field-emission scanning electron microscopy (FESEM, ZEISS Supra 40VP), X-ray diffraction (XRD, Shimadzu XRD-6000, Cu K-alpha radiation, wavelength 1.54 Å) and UV-Vis-NIR spectrophotometer (Cary 5000). The photocurrent was measured using UV photocurrent measurement unit (Keithley 2400) to investigate the response under UV lamp (365 nm, 750 μWcm<sup>-2</sup>).

### 3. RESULTS AND DISCUSSION

Figure 2(a and b) show the top view of the deposited TNAs and TNAs/PANI heterojunction at 10,000× magnification, respectively. A dense structure

and high surface-to-volume ratio of TNAs is clearly observed and uniformly grown over the whole surface area of FTO-coated glass substrate. The TNAs are in tetragonal shape with square top facets in average. Figure 2(a) also shows that the average nanorod diameter of the TNAs is approximately 120 nm. The deposited PANI thin film on TNAs (Figure 2(b)) increased the average nanorod diameter to approximately 150 nm. The result indicated that a relatively thin layer of PANI was deposited on the surface of each nanorod.

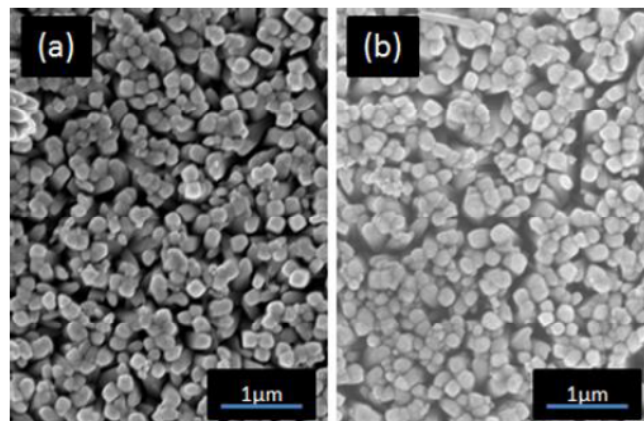


**Figure 2:** FESEM images of (a) TNAs, and (b) TNAs/PANI heterojunction at 10,000 × magnifications.

Figure 3 shows the XRD pattern of the deposited TNAs/PANI heterojunction on the FTO-coated glass substrate. All the diffraction peaks show the rutile phase of TiO<sub>2</sub> (JCPDS No. 01-072-1148). The (0 0 2) diffraction peak are relatively high to indicate the one-directional growth of TNAs. The diffraction peaks to represent the FTO are also visible in the pattern. However, no broad peak to represent PANI can be observed in the pattern, which indicates that the conductive polymer of PANI is relatively low crystallinity

in attribution to the repetition of benzenoid and quinoid rings in PANI chains [19, 20]. The result could also be attributed to the amorphous structure of PANI and the limitation of XRD measurement unit to detect low thickness layer of PANI film.

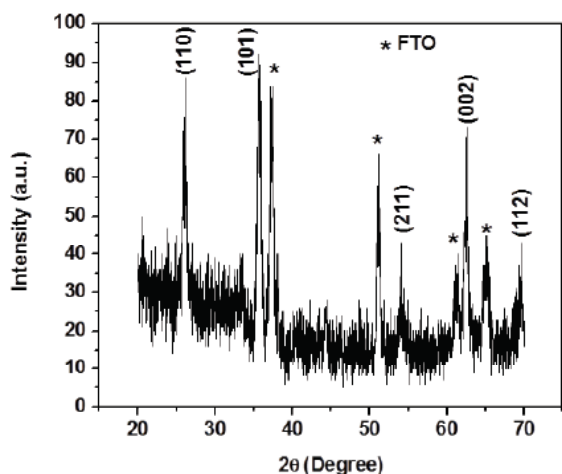


**Figure 3:** XRD pattern of the deposited TNAs/PANI heterojunction on FTO-coated glass substrate.

Figure 4 shows the optical absorbance spectrum of TNAs and TNAs/PANI heterojunction in 300–800 nm range. It can be seen that both TNAs and TNAs/PANI heterojunction have large absorption peaks at the 300–400 nm of UV range. TNAs on FTO-coated glass substrate has high absorption in UV range in attribution to its wide band gap energy of around 3.2 eV [21]. The result also shows that the absorbance of fabricated TNAs/PANI heterojunction is shifted to higher wavelength compared to the absorbance of TNAs in the UV region, due to the existence of PANI. The intensity of the absorbance was also increased in attribution to the light scattering effect on the thicker

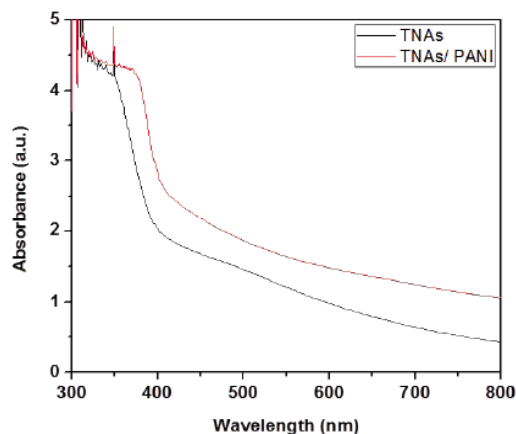


**Figure 4:** UV-vis absorbance spectrum of TNAs and TNAs/PANI heterojunction.

film of TNAs/PANI, compared to bare TNAs film. The result was also indicated that the synthesized and deposited TNAs/PANI on the substrate has stronger photocatalytic activity in UV region compared to visible region, which made it suitable for the application of UV photosensor.

Figure 5 shows the time-dependent photocurrent response of the fabricated TNAs/PANI heterojunction under UV irradiation (365 nm,  $750 \mu\text{W}/\text{cm}^2$ ) at various bias voltages. The signal pulses were generated by switching the UV source periodically to measure the photocurrent during “on” and “off” states. The minimum photocurrent during the “off” state is defined as the dark current from the baseline throughout the measurement. The abrupt change to the maximum value in average of the current during the “on” state from the “off” state is the total gain of photocurrent under the UV irradiation. The rise time was considered negligible throughout the whole measurement. The abrupt change of photocurrent may be due to the enhancement of charge carriers transportation within the solid-state structure of TNAs/PANI in which charge carriers are generated instantaneously through UV irradiation and the recombination of photo-generated charge carriers [22, 23].

The photocurrent response also exhibits that the measured dark current increases with increasing applied reverse bias of the heterojunction at 0.5–2.5 V. This result could be attributed to the increase of driving force from the external potential difference. The photocurrent also increases with increasing applied reverse bias to some extent under the UV irradiation during the “on” state. From the result, it can be seen that by far the greatest value of photocurrent is  $0.52 \mu\text{A}/\text{cm}^2$ , and the responsivity is 0.65 mA/W at the applied bias of 1.0 V. However, the photocurrent decreases with increasing applied reverse bias from 1.5 V onwards to some extent. The fabricated device from the deposited TNAs/PANI heterojunction using the introduced method is thereby made available for UV sensing purpose due to considerable high intensity, fast response and excellent reproducible characteristics.

The generation of photocurrent in the fabricated device could be attributed to the formation of internal potential difference at the heterojunction between the p-type PANI and n-type TNAs when it was irradiated with UV source. The generation of charge carriers through UV source also leads to a decrease in resistance [24], and therefore contributes to an increase in photocurrent.

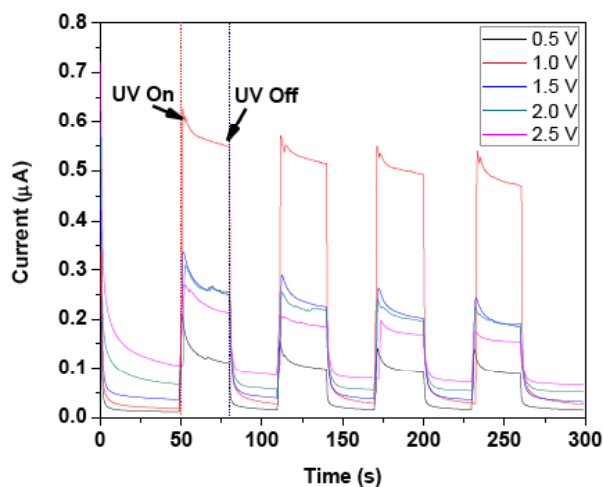


**Figure 5:** Photocurrent response under UV irradiation (365 nm,  $750 \mu\text{W}/\text{cm}^2$ ) at various bias voltages.

The external potential difference during the measurement offers a driving force to separate the photo-generated charge carriers, and prevents loss of electrons from the recombination of electron-hole pairs, while the electric force generated in between the heterojunction guides the electrons from the p-type PANI to the n-type TNAs and developing the total gain of photocurrent [25]. It is postulated that an increase in photocurrent may be due to the attraction of positive charge in the opposite junction to the photo-generated electrons.

## CONCLUSION

The present study was designed to determine the effect of p-type PANI on n-type TNAs in the fabrication of TNAs/PANI heterojunction-based UV photosensor using a novel and facile method. This study has shown that dark current increases with increasing applied reverse bias during the "off" state without the UV irradiation. The highest photocurrent of  $0.52 \mu\text{A}/\text{cm}^2$ , and responsivity of  $0.65 \text{ mA}/\text{W}$  was obtained at the applied bias of 1.0 V through the UV irradiation (365 nm,  $750 \mu\text{W}/\text{cm}^2$ ). The fabricated TNAs/PANI heterojunction device has shown a UV-catalytic activity and could be used to develop the application of UV photosensor and UV switching devices.

## ACKNOWLEDGEMENT

This work was financially supported by the Fundamental Research Grant Scheme 600-RMI/FRGS 5/3 (57/2015) from the Ministry of Education Malaysia. The authors also would like to thank the Faculty of Electrical Engineering (FKE), NANO-ElecTronic Centre

(NET), NANOSciTech Centre (NST), Research Management Centre (RMC) of University Teknologi MARA, Shah Alam, Malaysia (UiTM), the Ministry of Higher Education of Malaysia, and International Islamic University Malaysia (IIUM).

## REFERENCES

- [1] Hwang JD and Lin GS. "Single- and dual-wavelength photodetectors with MgZnO/ZnO metal-semiconductor-metal structure by varying the bias voltage," *Nanotechnology* 2016; 27: 375502. <https://doi.org/10.1088/0957-4484/27/37/375502>
- [2] Dali S, Mingpeng Y, Jie L and Shayla S. "An ultraviolet photodetector fabricated from  $\text{WO}_3$  nanodiscs/reduced graphene oxide composite material," *Nanotechnology* 2013; 24: 295701. <https://doi.org/10.1088/0957-4484/24/29/295701>
- [3] Li Q, Qiu T, Hao H, Zhou H, Wang T, Zhang Y *et al.*, "Rapid and on-site analysis of illegal drugs on the nano-microscale using a deep ultraviolet-visible reflected optical fiber sensor," *Analyst* 2012; 137: 1596-603. <https://doi.org/10.1039/c2an15953h>
- [4] Li X, Gao C, Duan H, Lu B, Pan X and Xie E. "Nanocrystalline  $\text{TiO}_2$  film based photoelectrochemical cell as self-powered UV-photodetector," *Nano Energy* 2012; 1: 640. <https://doi.org/10.1016/j.nanoen.2012.05.003>
- [5] Vigil E, Peter LM, Forcade F, Jennings JR, González B, Wang H *et al.*, "An ultraviolet selective photodetector based on a nanocrystalline  $\text{TiO}_2$  photoelectrochemical cell," *Sensors and Actuators A: Physical* 2011; 171: 87-92. <https://doi.org/10.1016/j.sna.2011.07.005>
- [6] Xiang WF, Yang PR, Wang AJ, Zhao K, Ni H and Zhong SX. "Vertical geometry ultraviolet photodetectors with high photosensitivity based on nanocrystalline  $\text{TiO}_2$  films," *Thin Solid Films* 2012; 520: 7144-7146. <https://doi.org/10.1016/j.tsf.2012.07.110>
- [7] Mamat MH, Malek MF, Hafizah NN, Khusairi Z, Musa MZ and Rusop M. "Fabrication of an ultraviolet photoconductive sensor using novel nanostructured, nanohole-enhanced, aligned aluminium-doped zinc oxide nanorod arrays at low immersion times," *Sensors and Actuators B: Chemical* 2014; 195(5): 609-622. <https://doi.org/10.1016/j.snb.2014.01.082>
- [8] Gao C, Li X, Zhu X, Chen L, Wang Y, Teng F *et al.*, "High performance, self-powered UV-photodetector based on ultrathin, transparent,  $\text{SnO}_2$ - $\text{TiO}_2$  core-shell electrodes," *Journal of Alloys and Compounds* 2014; 616: 510-515. <https://doi.org/10.1016/j.jallcom.2014.07.171>
- [9] Tian W, Zhang C, Zhai T, Li SL, Wang X, Liu J *et al.*, "Flexible Ultraviolet Photodetectors with Broad Photoresponse Based on Branched ZnS-ZnO Heterostructure Nanofilms," *Advanced Materials* 2014; 26: 3088-3093. <https://doi.org/10.1002/adma.201305457>
- [10] Xu Z, Han L, Lou B, Zhang X and Dong S. "High-performance BiOBr ultraviolet photodetector fabricated by a green and facile interfacial self-assembly strategy," *Nanoscale* 2014; 6: 145-150. <https://doi.org/10.1039/C3NR04496C>
- [11] Li X, Qi J, Zhang Q and Zhang Y. "Bias-tunable dual-mode ultraviolet photodetectors for photoelectric tachometer," *Applied Physics Letters* 2014; 104: 041108. <https://doi.org/10.1063/1.4863431>
- [12] Zou R, Zhang Z, Liu Q, Hu J, Sang L, Liao M *et al.*, "High Detectivity Solar-Blind High-Temperature Deep-Ultraviolet Photodetector Based on Multi-Layered (100) Facet-Oriented

- $\beta$ -Ga<sub>2</sub>O<sub>3</sub> Nanobelts," *Small* 2014; 10: 1848-1856.  
<https://doi.org/10.1002/smll.201302705>
- [13] Hussain AA, Pal AR and Patil DS. "An efficient fast response and high-gain solar-blind flexible ultraviolet photodetector employing hybrid geometry," *Applied Physics Letters* 2014; 104: 193301.  
<https://doi.org/10.1063/1.4876450>
- [14] Dao TD, Dang CTT, Han G, Hoang CV, Yi W, Narayanamurti V *et al.*, "Chemically synthesized nanowire TiO<sub>2</sub>/ZnO core-shell p-n junction array for high sensitivity ultraviolet photodetector," *Applied Physics Letters* 2013; 103: 193119.  
<https://doi.org/10.1063/1.4826921>
- [15] Yang S, Cui X, Gong J and Deng Y. "Synthesis of TiO<sub>2</sub>-polyaniline core-shell nanofibers and their unique UV photoresponse based on different photoconductive mechanisms in oxygen and non-oxygen environments," *Chemical Communications* 2013; 49: 4676-4678.  
<https://doi.org/10.1039/c3cc39157d>
- [16] Liu B and Aydil ES. "Growth of Oriented Single-Crystalline Rutile TiO<sub>2</sub> Nanorods on Transparent Conducting Substrates for Dye-Sensitized Solar Cells," *Journal of the American Chemical Society* 2009; 131: 3985-3990.  
<https://doi.org/10.1021/ja8078972>
- [17] Yusoff MM, Mamat MH, Malek MF, Suriani AB, Mohamed A, Ahmad MK *et al.*, "Growth of titanium dioxide nanorod arrays through the aqueous chemical route under a novel and facile low-cost method," *Materials Letters* 2016; 164: 294-298.  
<https://doi.org/10.1016/j.matlet.2015.11.014>
- [18] Zu X, Wang H, Yi G, Zhang Z, Jiang X, Gong J *et al.*, "Self-powered UV photodetector based on heterostructured TiO<sub>2</sub> nanowire arrays and polyaniline nanoflower arrays," *Synthetic Metals* 2015; 200(2): 58-65.  
<https://doi.org/10.1016/j.synthmet.2014.12.030>
- [19] Shi L, Wang X, Lu L, Yang X and Wu X. "Preparation of TiO<sub>2</sub>/polyaniline nanocomposite from a lyotropic liquid crystalline solution," *Synthetic Metals* 2009; 59: 2525-2529.  
<https://doi.org/10.1016/j.synthmet.2009.08.056>
- [20] Mostafaei A and Zolriasatein A. "Synthesis and characterization of conducting polyaniline nanocomposites containing ZnO nanorods," *Progress in Natural Science: Materials International* 2012; 22: 273-280.  
<https://doi.org/10.1016/j.pnsc.2012.07.002>
- [21] Xie Y, Wei L, Wei G, Li Q, Wang D, Chen Y *et al.*, "A self-powered UV photodetector based on TiO<sub>2</sub> nanorod arrays," *Nanoscale Research Letters* 2013; 8: 188.  
<https://doi.org/10.1186/1556-276X-8-188>
- [22] Li Y, Della Valle F, Simonnet M, Yamada I and Delaunay JJ. "High-performance UV detector made of ultra-long ZnO bridging nanowires," *Nanotechnology* 2009; 20: 045501.  
<https://doi.org/10.1088/0957-4484/20/4/045501>
- [23] Han Y, Wu G, Wang M and Chen H. "High efficient UV-A photodetectors based on monodispersed ligand-capped TiO<sub>2</sub> nanocrystals and polyfluorene hybrids," *Polymer* 2010; 51: 3736-3743.  
<https://doi.org/10.1016/j.polymer.2010.05.057>
- [24] Wu W, Bai S, Cui N, Ma F, Wei Z, Qin Y *et al.*, "Increasing UV Photon Response of ZnO Sensor with Nanowires Array," *Science of Advanced Materials* 2010; 2: 402-406.  
<https://doi.org/10.1166/sam.2010.1103>
- [25] Zhang Z, Shao C, Li X, Wang C, Zhang M and Liu Y. "Electrospun Nanofibers of p-Type NiO/n-Type ZnO Heterojunctions with Enhanced Photocatalytic Activity," *ACS Applied Materials & Interfaces* 2010; 2: 2915-2923.  
<https://doi.org/10.1021/am100618h>

Received on 15-05-2017

Accepted on 02-06-2017

Published on 15-06-2017

<http://dx.doi.org/10.15379/2408-977X.2017.04.01.02>© 2017 Yusoff *et al.*; Licensee Cosmos Scholars Publishing House.

This is an open access article licensed under the terms of the Creative Commons Attribution Non-Commercial License

(http://creativecommons.org/licenses/by-nc/3.0/), which permits unrestricted, non-commercial use, distribution and reproduction in any medium, provided the work is properly cited.